



## Cross section and resonance effects in photoemission from Sn-doped $\text{In}_2\text{O}_3(111)$

K.H.L. Zhang, D.J. Payne<sup>1</sup>, R.G. Egdell\*

Department of Chemistry, University of Oxford, Inorganic Chemistry Laboratory, South Parks Road, Oxford, OX1 3QR, UK

### ARTICLE INFO

#### Article history:

Received 3 August 2011

Received in revised form

18 October 2011

Accepted 6 November 2011

by D.D. Sarma

Available online 12 November 2011

#### Keywords:

A. Semiconductors

B. Epitaxy

D. Electronic band structure

E. Photoelectron spectroscopies

### ABSTRACT

Photoemission spectra of Sn-doped  $\text{In}_2\text{O}_3(111)$  have been measured using a range of photon energies between 40 and 1300 eV. The intensity of structure at the bottom of the valence band associated with states of mixed Sn 5s/O 2p character increases with increasing photon energy relative to that of states of more dominantly O 2p character at the top of the valence band, as expected from one electron ionisation cross sections. In addition a pronounced resonance in the intensity of a weak conduction band feature is observed around the In 4p core threshold.

© 2011 Elsevier Ltd. All rights reserved.

### 1. Introduction

Tin doped indium oxide, widely known as indium tin oxide or ITO, is one of the most important of all transparent conducting oxides with important applications as a window electrode in liquid crystal and other display devices and in the many designs of solar cell which require a transparent electrode [1–3]. Indium oxide itself adopts the body centred cubic bixbyite structure (space group  $Ia\bar{3}$ ). This is based on a  $2 \times 2 \times 2$  superstructure of fluorite with ordered removal of 25% of the oxygen ions. The onset of strong optical absorption in  $\text{In}_2\text{O}_3$  is found around 3.75 eV [4], which is almost 1 eV greater than the onset of weak optical absorption [5] now known to be associated with direct but dipole forbidden transitions [6]. The bandgap of 2.9 eV [7] for  $\text{In}_2\text{O}_3$  is intermediate between the neighbouring oxides CdO and  $\text{SnO}_2$  which have respectively a lowest energy indirect gap estimated to be 1.2 eV [8–10] and a direct but forbidden gap of 3.62 eV [11].

In the ionic model limit the  $\text{O}^{2-}$  ions of  $\text{In}_2\text{O}_3$  have an electron configuration  $2p^6$  while the electron configuration of  $\text{In}^{3+}$  is  $4d^{10}5s^05p^0$ . In terms of this model the valence band is composed of O 2p states and the conduction band derives from In 5s states. However, band structure calculations suggest that  $\text{In}_2\text{O}_3$  is a highly covalent material, with pronounced In 5s and In 5p character found respectively toward the bottom and the middle of the

valence band [12,13]. Conversely there is corresponding O 2p character in the conduction band. Photoemission spectroscopy using a variable incident photon energy provides one means of unravelling the contributions of differing atomic orbitals to the occupied states in a solid and indeed this approach has been used to study the electronic structure of both CdO [14] and  $\text{SnO}_2$  [15,16]. Somewhat surprisingly we are unaware of corresponding work using a series of photon energies to study the electronic structure of  $\text{In}_2\text{O}_3$ . In the current paper we therefore present a study of Sn-doped  $\text{In}_2\text{O}_3$  by photoemission spectroscopy using a range of photon energies between 40 and 1300 eV. The experimental results provide evidence of In 5s character both at the bottom of the valence band and in the conduction band.

### 2. Materials and methods

Epitaxial thin films of undoped and Sn-doped  $\text{In}_2\text{O}_3$  were grown on  $1 \text{ cm} \times 1 \text{ cm}$  Y-stabilized  $\text{ZrO}_2(111)$  substrates in an ultrahigh vacuum oxide MBE system (SVT, USA) with a base pressure of  $5 \times 10^{-10}$  mbar ( $5 \times 10^{-8}$  Pa). This incorporated a hot lip indium Knudsen cell, a conventional Sn Knudsen cell and a radio frequency (RF) plasma oxygen atom source operated at 200 mW RF power with an oxygen background pressure of  $3 \times 10^{-5}$  mbar ( $3 \times 10^{-3}$  Pa). Substrates were heated radiatively using a graphite filament. The nominal growth rate was  $0.035 \text{ nm s}^{-1}$ , as calibrated from the film thickness derived from HRTEM measurements. The Y-ZrO<sub>2</sub> substrates were cleaned by exposure to the oxygen atom beam at a nominal substrate temperature of 900 °C. Films were then grown to a thickness of 210 nm at a substrate temperature of 700 °C. *In situ* display LEED

\* Corresponding author. Tel.: +44 1865 285157.

E-mail address: [Russell.egdell@chem.ox.ac.uk](mailto:Russell.egdell@chem.ox.ac.uk) (R.G. Egdell).

<sup>1</sup> Present address: Department of Materials, Imperial College London, Exhibition Road, London SW7 2AZ, UK.

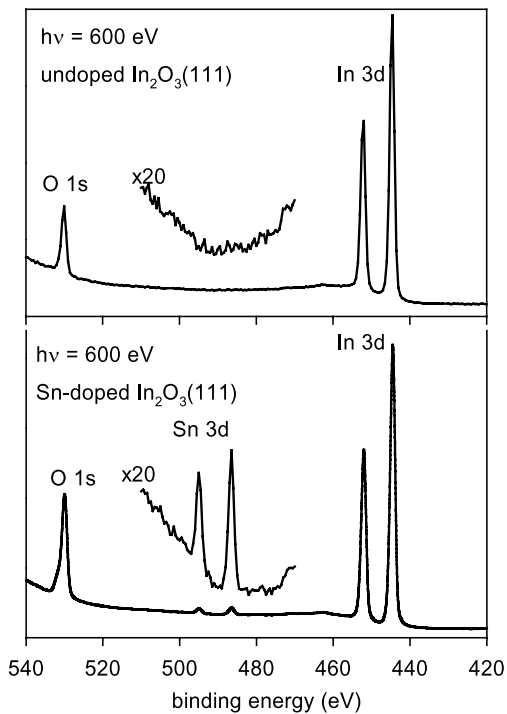


**Fig. 1.** Photoemission spectra of undoped  $\text{In}_2\text{O}_3(111)$  and Sn-doped  $\text{In}_2\text{O}_3(111)$  excited at  $h\nu = 600$  eV encompassing In 3d, Sn 3d and O 1s core levels.

was carried out in an analysis chamber connected to the growth chamber, which revealed a well ordered  $(1 \times 1)$  reconstruction. The carrier concentrations determined by Hall effect measurements were respectively  $2 \times 10^{19}$  and  $6 \times 10^{20} \text{ cm}^{-3}$  for the nominally

undoped and doped samples. Photoemission measurements were performed on beamline I311 of the MAX II synchrotron housed at MAXLAB, Lund, Sweden. The beamline is based on a 48.5 period undulator and operates in an energy range between 40 and 1500 eV. The ultrahigh vacuum end station incorporates a sample preparation chamber including facilities for sample heating, whilst the analysis chamber houses a Scienta SES200 spherical sector electron energy analyser. Clean ordered surfaces are easily regenerated by heating the samples to  $700^\circ\text{C}$  for several hours [17]. Some additional offline measurements were performed at  $h\nu = 1486.6$  eV in a Scienta ESCA 300 electron spectrometer incorporating a monochromatised rotating anode X-ray source and a 300 mm mean radius hemispherical energy analyser with parallel electron detection system.

### 3. Results and discussion

Photoemission spectra of undoped  $\text{In}_2\text{O}_3(111)$  and of Sn-doped  $\text{In}_2\text{O}_3(111)$  excited at  $h\nu = 600$  eV in the region of the In 3d, Sn 3d and O 1s core lines are shown in Fig. 1. As expected the spectrum of the doped samples contains a weak but well defined Sn 3d spin-orbit doublet associated with the Sn dopant: after correction for ionisation cross sections the ratio of concentrations  $\text{In}/(\text{In} + \text{Sn})$  in the near surface region probed by XPS is estimated to be 0.022. Assuming that there is no compensation of Sn by interstitial oxygen, this corresponds to a carrier concentration of  $6.8 \times 10^{20} \text{ cm}^{-3}$ , in good agreement with the Hall measurements. This is sufficient to bring about degenerate doping of the  $\text{In}_2\text{O}_3$  and thus to populate the conduction band. In turn this ensures that samples are sufficiently conducting that there are no problems with sample charging during photoemission experiments. The measurements performed on the undoped sample were more restricted due to sample charging problems.

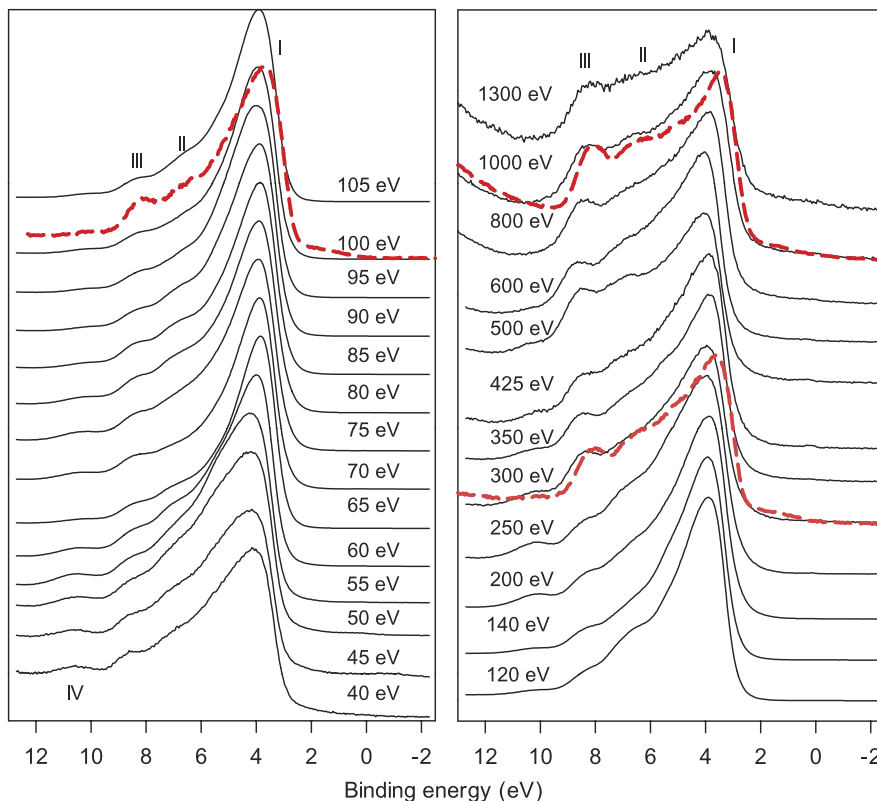


**Fig. 2.** Solid lines: valence band photoemission spectra of Sn-doped  $\text{In}_2\text{O}_3(111)$  excited at the photon energies indicated. The overlaid spectra shown with dashed lines (red online) at 100, 300 and 1000 eV photon energy are from undoped  $\text{In}_2\text{O}_3(111)$ . (For interpretation of the references to colour in this figure legend, the reader is referred to the web version of this article.)

Photoemission spectra of Sn-doped  $\text{In}_2\text{O}_3(111)$  excited at photon energies between 40 and 1300 eV are shown in Fig. 2. The spectra of undoped  $\text{In}_2\text{O}_3(111)$  are very similar (as shown in the overlays in Fig. 2 for selected photon energies), although doping evidently produces a small shift to higher binding energy as will be discussed below. Three main features may be identified in the spectra: a peak with maximum intensity at around 3.9 eV binding energy along with less prominent shoulders at 6.6 and 8.5 eV binding energy. These are labelled as I, II and III in the figure. A weaker feature labelled IV with a binding energy of 10.5 eV is apparent in some spectra, especially those excited at low photon energies between 40 and 60 eV. Partial densities of states derived from bandstructure calculations [13] (Fig. 3) reveal that the states associated with peak I are of dominant O 2p character (with a small admixture of shallow core In 4d states). By contrast the states associated with band III have large contribution from In 5s states as well as O 2p states. Similarly the intermediate peak II is a mixture of In 5p and O 2p states. The very weak peak IV is probably associated with Sn 5s states hybridised with O 2p states.

The main change in the spectra found upon increasing the photon energy is that the intensity of the peak III and to a lesser extent peak II increases relative to peak I. This may be understood in terms of changes in ionisation cross sections illustrated in Fig. 4. This figure shows that both O 2p and In 5s one electron cross sections have maxima below 100 eV and thereafter decrease monotonically with increasing photon energy. However the decay of the O 2p cross sections is much more pronounced than for the In 5s states so that the In 5s/O 2p cross section ratio increases with increasing photon energies and above about 500 eV the In 5s cross section is bigger than O 2p: somewhat surprisingly the standard tabulation of cross sections due to Yeh and Lindau [18] does not give values for one ionisation cross sections of In 5p states, although from consideration of cross sections for Sn 5s and 5p states and from values of cross sections above 1000 eV tabulated by Scofield [19] we may infer that the In 5p cross section is about half that of In 5s states in the energy range between 100 and 1000 eV, thus explaining the variations in intensity of band II.

A weak feature straddling the Fermi energy is observed for photon energies between 60 and 110 eV (Fig. 5): unfortunately at higher photon energies this very weak structure is generally obscured by photoemission arising from second order synchrotron radiation. However structure at the Fermi energy can also be observed in spectra excited with conventional monochromatic Al  $K\alpha$  radiation with  $h\nu = 1486.6$  eV, as shown in Fig. 6. These spectra reveal that this structure is even weaker (but not zero) for the nominally undoped sample. The weak feature may therefore be associated with partial filling of the conduction band due to Sn doping. As discussed in detail elsewhere [13] doping produces a shift to higher binding energy due to an upward shift of the Fermi level within the conduction band. The non-vanishing intensity in the nominally undoped sample arises from downward band bending at the surface with consequent carrier accumulation [7,20].

This intensity of the conduction band structure declines in intensity between 70 and 80 eV photon energy but then shows a pronounced intensity enhancement in the energy range between 85 and 95 eV before decreasing again. The conduction band states in Sn-doped  $\text{In}_2\text{O}_3$  are of mixed Sn 5s/In 5s and O 2p character. The rapid variation in intensity is not predicted by the computed one electron ionisation cross sections but is instead attributed to a Fano anti-resonance/resonance line shape linked to the In 4p core threshold. The In 4d, In 4p and In 4s core level spectra of the sample excited at 1486.6 eV photon energy are shown in Fig. 7. The In 4p core level appears as a very broad feature centred around 80 eV binding energy. The large width arises from many electron effects which allow 4p hole states to mix with excited 4d hole

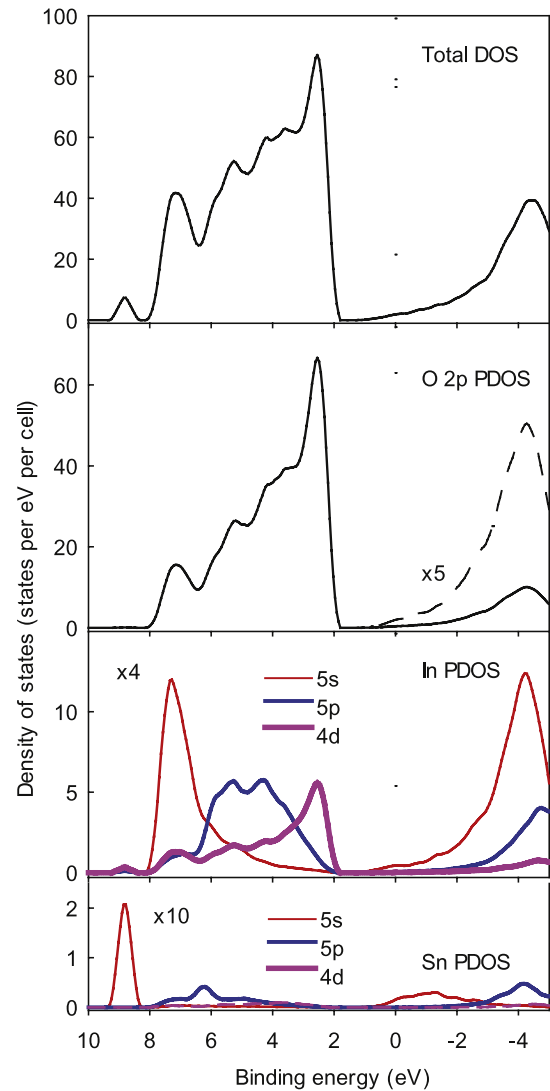
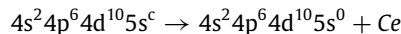
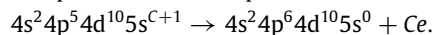
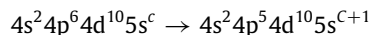


Fig. 3. Full and partial densities of states for Sn-doped  $\text{In}_2\text{O}_3$ . Source: Adapted from Ref. [13].

states—in the nearby element tellurium this leads to a complete breakdown in the one electron picture for a core hole [21]. Using a notional configuration  $5s^c$  to represent partial occupancy of the In 5s derived conduction band, the Fano intensity profile is then attributed to interference between the direct photoemission channel:



and the channel where resonant photoexcitation is followed by Coster–Krönig decay:



Very similar resonance structure has been observed [16] in photoemission from bandgap states with significant Sn 5s in reduced  $\text{SnO}_2$ , although as expected the peaks and the dip are shifted to higher photon energy than observed here owing to the greater nuclear charge on Sn as compared with In.

In summary photoemission spectra of Sn-doped  $\text{In}_2\text{O}_3$  have been measured over a range of photon energies between 40 and 1300 eV. The spectra provide evidence for Sn 5s character both in the states that go to make up the conduction band and in states at the bottom of the valence band. The results complement earlier comparable work on CdO [14] and  $\text{SnO}_2$  [16].

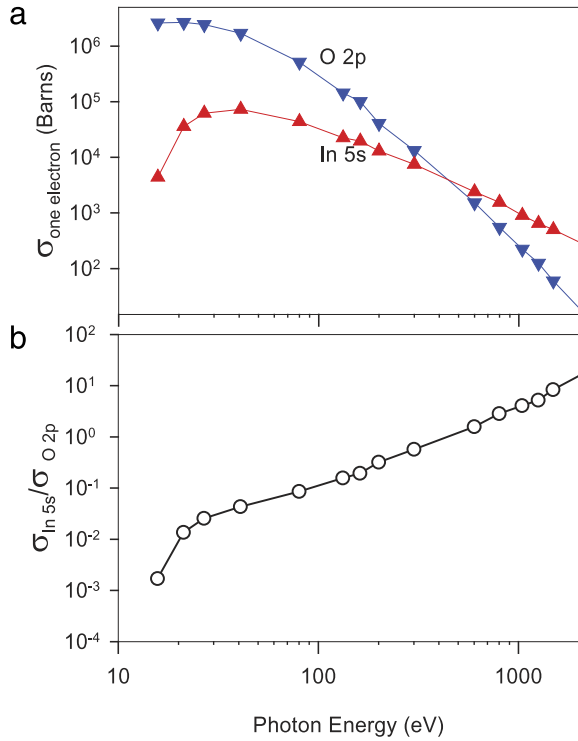


**Fig. 4.** (a) One electron ionisation cross sections for O 2p and In 5s states calculated by Yeh and Lindau as a function of photon energy. (b) One electron cross section ratio  $\sigma_{\text{In5s}}/\sigma_{\text{O 2p}}$  as a function of photon energy.

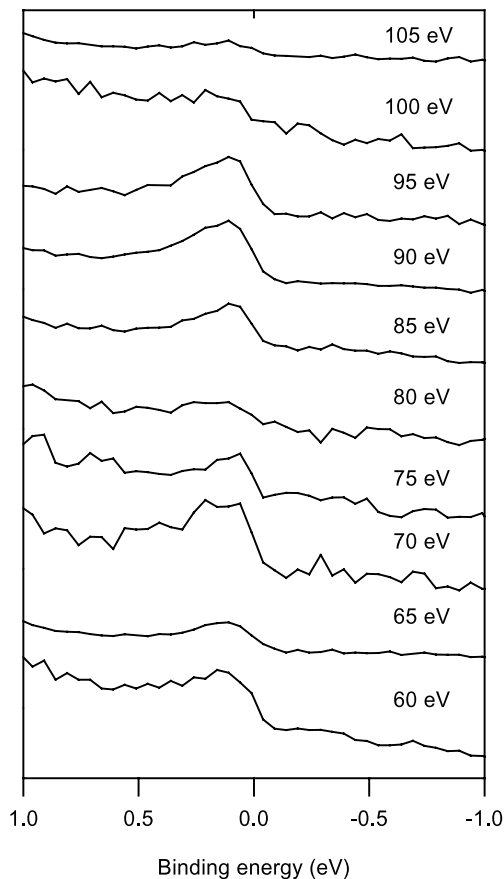


**Fig. 5.** Expansion of the conduction band region in photoemission spectra of Sn-In<sub>2</sub>O<sub>3</sub>(111) in the photon energy regime between 60 and 105 eV.

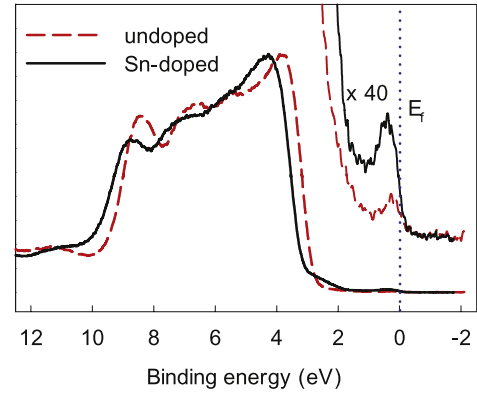


**Fig. 6.** Valence band and conduction band spectra of nominally undoped and 2.2% Sn-doped In<sub>2</sub>O<sub>3</sub>(111) excited at 1486.6 eV photon energy using a conventional AlK $\alpha$  source.

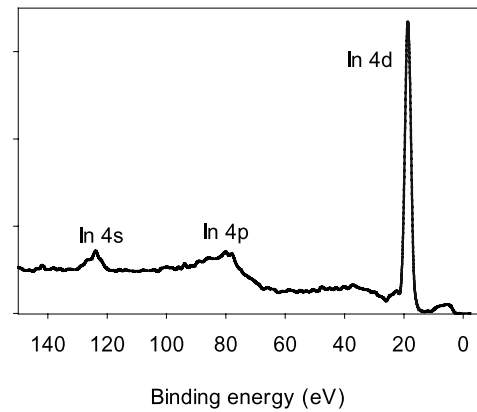


**Fig. 7.** Photoemission spectra of Sn-In<sub>2</sub>O<sub>3</sub>(111) in region of In 4d, In 4p and In 4s core levels measured at  $h\nu = 1486.6$  eV.

## Acknowledgments

The oxide MBE programme was supported by EPSRC grant GR/S94148. KHLZ is grateful to Oxford University for the award of a Clarendon Scholarship. DJP is grateful to Christchurch, Oxford for a Junior Research Fellowship. This work was supported by the UK Royal Society Research Grant RG080399.

## References

- [1] C.G. Granqvist, A. Hultaker, *Thin Solid Films* 411 (2002) 1.
- [2] D.S. Ginley, H. Hosono, D.C. Paine (Eds.), *Handbook of Transparent Conductors*, Springer, New York, 2010.
- [3] H. Hosono, *Thin Solid Films* 515 (2007) 6000.
- [4] I. Hamberg, C.G. Granqvist, K.F. Berggren, B.E. Sernelius, L. Engstrom, *Phys. Rev. B* 30 (1984) 3240.
- [5] R.L. Weiher, R.P. Ley, *J. Appl. Phys.* 37 (1966) 299.
- [6] A. Walsh, J.L.F. Da Silva, S.H. Wei, C. Korber, A. Klein, L.F.J. Piper, A. DeMasi, K.E. Smith, G. Panaccione, P. Torelli, D.J. Payne, A. Bourlange, R.G. Egdell, *Phys. Rev. Lett.* 100 (2008) 167402.
- [7] P.D.C. King, T.D. Veal, F. Fuchs, C.Y. Wang, D.J. Payne, A. Bourlange, H. Zhang, G.R. Bell, V. Cimalla, O. Ambacher, R.G. Egdell, F. Bechstedt, C.F. McConville, *Phys. Rev. B* 79 (2009) 205211.
- [8] Y. Dou, R.G. Egdell, T. Walker, D.S.L. Law, G. Beamson, *Surf. Sci.* 398 (1998) 241.
- [9] Y. Dou, T. Fishlock, R.G. Egdell, D.S.L. Law, G. Beamson, *Phys. Rev. B* 55 (1997) 13381.
- [10] C. McGuinness, C.B. Stagescu, P.J. Ryan, J.E. Downes, D.F. Fu, K.E. Smith, R.G. Egdell, *Phys. Rev. B* 68 (2003) 165104.
- [11] D. Frohlich, R. Kenklies, R. Helbig, *Phys. Rev. Lett.* 41 (1978) 1750.
- [12] P. Erhart, A. Klein, R.G. Egdell, K. Albe, *Phys. Rev. B* 75 (2007) 153205.

- [13] C. Korber, V. Krishnakumar, A. Klein, G. Panaccione, P. Torelli, A. Walsh, J.L.F. Da Silva, S.H. Wei, R.G. Egdell, D.J. Payne, *Phys. Rev. B* 81 (2010) 165207.
- [14] Y. Dou, R.G. Egdell, D.S.L. Law, N.M. Harrison, B.G. Searle, *J. Phys.: Condens. Matter* 10 (1998) 8447.
- [15] J.M. Themlin, R. Sporken, J. Darville, R. Caudano, J.M. Gilles, R.L. Johnson, *Phys. Rev. B* 42 (1990) 11914.
- [16] M. Sinner-Hettenbach, M. Gothelid, T. Weiss, N. Barsan, U. Weimar, H. von Schenck, L. Giovanelli, G. Le Lay, *Surf. Sci.* 499 (2002) 85.
- [17] K.H.L. Zhang, D.J. Payne, R.G. Palgrave, V.K. Lazarov, W. Chen, A.T.S. Wee, C.F. McConville, P.D.C. King, T.D. Veal, G. Panaccione, P. Lacovig, R.G. Egdell, *Chem. Mater* 21 (2009) 4353.
- [18] J.J. Yeh, I. Lindau, *At. Data Nucl. Data Tables* 32 (1985) 1.
- [19] J. Scofield, Lawrence Livermore National Laboratory Report No. UCRL-51326, 1973.
- [20] P.D.C. King, T.D. Veal, D.J. Payne, A. Bourlange, R.G. Egdell, C.F. McConville, *Phys. Rev. Lett.* 101 (2008) 116808.
- [21] G. Wendin, M. Ohno, *Phys. Scr.* 14 (1976) 148.